

1 Atmospheric deposition of organic matter at a remote site in the 2 Central Mediterranean Sea: implications for marine ecosystem

3 Yuri Galletti¹, Silvia Becagli², Alcide di Sarra³, Margherita Gonnelli¹, Elvira Pulido-Villena⁴,
4 Damiano M. Sferlazzo³, Rita Traversi², Stefano Vestri¹, Chiara Santinelli¹

5 ¹CNR, Biophysics Institute, Pisa, Italy

6 ²Department of Chemistry "Ugo Schiff", University of Florence, Italy

7 ³Laboratory for Observations and Measurements for the Environment and Climate (SSPT-PROTER-OEM), ENEA,
8 Rome, Italy

9 ⁴Institut Méditerranéen d'Océanologie, MIO - Marseille, France

10
11 *Correspondence to:* Yuri Galletti (yuri.galletti@pi.ibf.cnr.it)

12
13 **Abstract.** Atmospheric fluxes of dissolved organic matter (DOM) were studied for the first time at the Island of
14 Lampedusa, a remote site in the Central Mediterranean Sea (Med Sea), between March 19th 2015 and April 1st 2017.
15 The main goals of this study were: to quantify total atmospheric deposition of DOM in this area and to evaluate the
16 impact of Saharan dust deposition on DOM dynamics in the surface waters of the Mediterranean Sea. Our data show
17 high variability in DOM deposition rates, without a clear seasonality, and a dissolved organic carbon (DOC) input from
18 the atmosphere of 120.7 mmol DOC m⁻² y⁻¹. Over the entire time-series, the average dissolved organic phosphorous
19 (DOP) and dissolved organic nitrogen (DON) contributions to the total dissolved pools were 40% and 26%,
20 respectively. The data on atmospheric elemental ratios also show that each deposition event is characterized by a
21 specific elemental ratio, suggesting a high variability in DOM composition and the presence of multiple sources. This
22 study indicates that the organic substances, transported by Saharan dust at Lampedusa, mainly come from a natural sea
23 spray, and that Saharan dust can be an important carrier of organic substances, even though the load of DOC associated
24 with dust is highly variable. Our estimates suggest that atmospheric input has a larger impact to the Med Sea than to the
25 global ocean. Further, DOC fluxes from the atmosphere to the Med Sea can be up to 6-fold larger than total river input.
26 Longer time series, combined with modelling would greatly improve our understanding of the response of DOM
27 dynamics in the Med Sea to the change in aerosol deposition pattern due to the effect of climate change.

28 29 1. Introduction

30 The Mediterranean Sea (Med Sea) is the largest semi-enclosed basin and one of the most oligotrophic areas of the
31 world's oceans. It is very sensitive to natural variations in the atmosphere-ocean interactions (Mermex group, 2011).
32 Organic matter and nutrients of natural and anthropogenic origin, are continuously exchanged between the ocean and
33 the atmosphere, affecting biogeochemical cycles and the marine ecosystem. The Med Sea receives anthropogenic
34 aerosols from the northern regions, which are characterized by the presence of important industrial sites, representing
35 relevant sources of organic substances to the atmosphere (Guerzoni and Chester, 1996). Industrial pollution can also be
36 originated from the North Africa as shown in the work by Rodríguez et al. (2011). In addition, the Sahara desert is an
37 intermittent source of mineral dust, that can transport nutrients and organic carbon to the Basin (Goudie and Middleton,
38 2001; Prospero et al., 2005; Vincent et al., 2016). Atmospheric deposition of nutrients (N and P) strongly influences the
39 marine biogeochemical cycles of the Med Sea, it has therefore received increased attention in the last 30 years (Migon
40 et al., 1989; Herut et al., 2002; Ridame and Guieu, 2002; Markaki et al., 2003, 2010; Pulido-Villena et al., 2008;
41 Izquierdo et al., 2012; Djaoudi et al., 2018). Compared to inorganic nutrients, there is still very few data on the

42 atmospheric deposition of Dissolved Organic Carbon (DOC) to the surface ocean, both at the local and global scale.
43 Organic carbon can be removed from the atmosphere through wet and dry deposition (Iavorivska et al., 2016). At the
44 global scale, wet deposition transfers about 306-580 Tg DOC yr⁻¹ to the surface of the Earth (Willey et al., 2000;
45 Kanakidou et al., 2012). These values correspond to almost half of the DOC delivered to the oceans by rivers annually
46 (IPCC, 2014). Atmospheric deposition of organic carbon can therefore affect regional C cycling (Yan and Kim, 2012;
47 Decina et al., 2018). In addition, the expected increase in ocean stratification due to the global warming will enhance
48 the impact of atmospheric inputs in the surface ecosystem (Kanakidou et al., 2012). The magnitude of atmospheric
49 DOC inputs to open waters and the importance of its role in the carbon cycle highlight the need for a better and robust
50 estimation of DOC deposition.

51 In the last years, a few studies have reported data on atmospheric deposition of DOC to the Med Sea. Total (dry + wet)
52 atmospheric deposition was studied in North-Western Med Sea in 2006 (Pulido-Villena et al., 2008) and in 2015
53 (Djaoudi et al., 2018) with contrasting results. In the first study, the highest DOC flux was observed during a Saharan
54 dust storm, suggesting a combination of heterogeneous reactions between organic matter and mineral dust in the
55 troposphere. In the second study, a Saharan rain event coincided with a minimum in DOC input, suggesting little
56 organic matter in aerosols (Djaoudi et al., 2018). These studies were conducted in coastal areas affected by human
57 activities. Direct measurements of total OC (TOC) in rainwater were carried out at the island of Crete (Economou and
58 Mihalopoulos, 2002). This study did not take into consideration dry deposition. None of the papers cited has studied
59 atmospheric inputs in remote sites, far from possible pollution sources and/or large cities.

60 The main goals of this study are: (1) to quantify total atmospheric deposition of DOC, DON and DOP at the island of
61 Lampedusa, representative of the remote marine environment in the central Med Sea; (2) to investigate the contribution
62 of natural and anthropogenic sources in atmospheric DOC; (3) to estimate the impact of atmospheric deposition on
63 marine ecosystem.

64

65 **2. Materials and methods**

66 **2.1 Sampling site**

67 Bulk atmospheric deposition (dry and wet) was collected at the Station for Climate Observations (35.52°N, 12.63°E),
68 maintained by ENEA, the Italian National Agency for New Technologies, Energy and Sustainable Economic
69 Development, on the island of Lampedusa, Italy (Fig. 1; <http://www.lampedusa.enea.it/>).

70 Lampedusa is located in an ideal position for the study of atmospheric DOC fluxes to the open Med Sea. It is flat and
71 far from large islands or continental areas and from relevant pollutant sources. Precipitation shows a significant
72 interannual variability and is concentrated in autumn and winter, with a maximum in October. Intense precipitation
73 events, which are relatively infrequent, are generally associated with frontal passages and winds from the Northern
74 sectors. Very dry conditions characterize late spring and summer. Although it is a remote marine environment,
75 influences from ship traffic emissions (Becagli et al., 2012, 2017), volcanic aerosols (Sellitto et al., 2017), forest fires
76 (Pace et al., 2005), and regional pollution (Pace et al., 2006) have been documented.

77 In addition to deposition, PM₁₀ (particulate matter with aerodynamic equivalent diameter lower than 10 µm) amount and
78 chemical composition analyses, routinely performed at Lampedusa, are used in this study.

79

80 **2.2. Atmospheric deposition sampler**

81 The sampler (Fig. 1) was positioned on the roof of the ENEA climatic station located on a 45 m a.s.l. plateau on the
82 north-eastern coast of Lampedusa. A total of 41 samples were collected between March 19th 2015 and April 1st 2017,
83 every 15 days or immediately after strong rain or dust storm events. Due to logistic constraints, 9 sampling periods were
84 longer than 20 days. The deposition sampler is similar to those successfully employed in previous studies (Pulido-
85 Villena et al., 2008; Markaki et al. 2010; De Vicente et al., 2012). It is composed of a 10 L polycarbonate bottle, with a
86 polyethylene funnel attached on the top; a 20 µM mesh covers the funnel stem in order to prevent contamination by
87 insects or organic debris. For wet deposition, the amount of water in the sampler was weighted and transferred to 250
88 ml polycarbonate bottles and immediately frozen. Dry deposition was sampled by rinsing the collector with 250 mL of
89 ultrapure MilliQ water, that was transferred into 250 ml polycarbonate bottles and immediately frozen. A detailed
90 description of sampling periods, deposition types, and collected volumes is reported in Table 1.

91 For DOC, DON and DOP analysis, samples were thawed and filtered through a sterile 0.2 µm Nylon filter pre-washed
92 with 300 ml of ultrapure water to avoid any contamination. Filtered samples were frozen until the analysis. Before the
93 analysis, samples were brought to room temperature (24 °C).

94

95 **2.3 DOC analysis**

96 DOC analysis were carried out on a Shimadzu TOC-VCSN, equipped with a quartz combustion column filled with
97 1.2% Pt on alumina pillows of ~2 mm diameter. Samples were first acidified with 2N HCl and bubbled for 3 min with
98 CO₂-free ultra-high purity air in order to remove the inorganic carbon. Replicate injections were performed until the
99 analytical precision was lower than 1%. A five-point linear calibration curve was determined with standard solutions of
100 potassium hydrogen phthalate in the same concentration range as the samples (40-400 µM). The system blank was
101 measured every day at the beginning and the end of analyses using low-carbon Milli-Q water (<3 µM C). Instrument
102 accuracy was assessed every day by analyzing DOC Consensus Reference Material (CRM), kindly provided by Prof. D.
103 Hansell, with a nominal value of 41-44 µM (batch 15 Lot #07-15) (Hansell, 2005). The average DOC concentration in
104 the CRM measured in our laboratory during the period of the analysis was 42.8±1.2 (n=15).

105

106 **2.4 DOP and DON analysis**

107 Twenty-six out of 41 samples were analyzed for dissolved organic nitrogen (DON) and phosphorous (DOP). The
108 samples were collected between March 19th 2015 and November 3rd 2016.

109 DON was estimated by subtracting the dissolved inorganic nitrogen (DIN) from the total dissolved N (TDN). DIN and
110 TDN were analyzed by conventional automated colorimetric procedure (CACP) according to Aminot and Kerouel
111 (2007) with an estimated limit of detection of 0.02 µM. TDN was analyzed after persulfate wet-oxidation (Pujo-Pay et
112 al., 1997).

113 DOP concentrations were determined by subtracting the inorganic form (soluble reactive phosphorus, SRP) from the
114 total dissolved P. SRP was measured spectrophotometrically after Murphy and Riley (1962) with a limit of detection of
115 0.02 µM and an analytical precision of 7% at 0.1 µM. Total dissolved P (TDP) was measured as SRP after UV
116 digestion (Armstrong et al., 1966). The photooxidation technique included a 2 hours UV treatment in a Metrohm® 705
117 UV digester with a digestion efficiency of 85 ± 3 %, assessed on a 1 µM solution of β-glycerol-phosphate.

118

119 **2.5 DOC, DON and DOP fluxes**

120 DOC, DON and DOP fluxes were calculated using the following formula:

$$121 \quad X_{\text{Flux}} = \frac{X \cdot V}{A \cdot d} \quad (1)$$

122 where X is the concentration measured in the sample (μM), V is the volume (L) of rain collected by the sampler or the
123 volume of Milli-Q water (0.25 L) used to rinse the collector in case of dry deposition, A is the area of the funnel
124 (0.1018 m^2), and d is the length of the sampling period expressed in days.

125

126 **2.6 Ions and metals content in the deposition samples**

127 Soluble ions metals were measured on samples filtered on quartz filters. These filters have low blank levels for metals
128 and ions (Ca, Na, Al and Pb) both in the soluble and particulate fraction. Immediately after filtration the samples were
129 divided in two portions, used for measurements of ionic and metal content, respectively. Samples for the determination
130 of metal were spiked with 0.1 mL of sub-boiled distilled (s.b.) HNO_3 to preserve the metals in their soluble form.
131 Samples were keep refrigerated at $+4^\circ\text{C}$ until the analysis. Ions were determined in solution by ion chromatography as
132 reported in Becagli et al. (2011).

133 The particulate fraction of the deposition was extracted from the quartz filter through the solubilisation procedure
134 reported in the EU EN14902 (2005) for aerosol samples. The extraction procedure was performed in a microwave oven
135 at 220°C by sub-boiling distilled HNO_3 and 30% ultra-pure H_2O_2 for 25 minutes.

136 Metals in both soluble and particulate fractions were measured by means of an Inductively Coupled Plasma Atomic
137 Emission Spectrometer (ICP-AES, Varian 720-ES) equipped with an ultrasonic nebulizer (U5000 ATC, Cetac
138 Technologies Inc.). Daily calibration standards (internal standard: 1 ppm Ge) were used for quantification.

139

140 **2.7 PM_{10} analysis**

141 PM_{10} is sampled on a daily basis at the island of Lampedusa (Becagli et al., 2013; Marconi et al., 2014; Calzolari et al.,
142 2015) by using a low-volume dual-channel sequential sampler (HYDRA FAI Instruments) equipped with two PM_{10}
143 sampling heads, operating at constant flow of $2.3 \text{ m}^3/\text{h}$ in accord with the European rules for aerosol monitoring (UNI
144 EN12341). Aerosol is collected on 47 mm diameter Teflon filters (PALL Gelman) having $2 \mu\text{m}$ nominal porosity but
145 certified to have 99% retention efficiency for $0.3 \mu\text{m}$ diameter particles. The PM_{10} mass was determined by weighting
146 the Teflon filters before and after sampling with an analytical balance in controlled conditions of temperature ($20 \pm 1^\circ\text{C}$)
147 and relative humidity ($50 \pm 5\%$). The estimated error on PM_{10} mass is around 1% at $30 \mu\text{g m}^{-3}$ in the routine sampling
148 conditions. A quarter of each Teflon filter was extracted using MilliQ water (about 10 ml, accurately evaluated by
149 weighing) in ultrasonic bath for 15 min, and the ionic content was determined by ion chromatography as for deposition
150 samples (Becagli et al. 2011). Another quarter of the Teflon filter was used for the determination of metals in the
151 atmospheric particles as described for the deposition samples.

152

153 **2.8 Enrichment factor**

154 In order to obtain information on DOM sources, DOM concentrations were compared to concentration of Al, Na and
155 the enrichment factor for Pb, EF(Pb), in the deposition samples as markers of crustal, sea spray and anthropic source
156 respectively.

157 The enrichment factor (EF) with respect to crustal sources of Pb, V and Ni were calculated by using Al as marker for
158 crustal aerosol. The following equation (Eq. 1) is used for EF calculation:

159

$$EF X = \frac{\left(\frac{X}{Al}\right)_{\text{sample}}}{\left(\frac{X}{Al}\right)_{\text{crust}}} \quad (2)$$

160

161

162

163

164

165

3. Results

166

3.1 DOC atmospheric fluxes

167

168

169

Atmospheric fluxes of DOC ranged between 0.06 and 1.78 mmol C m⁻² day⁻¹, with high variability. The overall sampling lasted for 746 days. The deposition was lower than 0.2 mmol DOC m⁻² d⁻¹ (Fig. 2 and Table 2) in half of the sampling days (52%).

170

171

172

173

174

175

176

In 2015, the lowest deposition rates (<0.1 C m⁻² d⁻¹) were measured in July (Lmp09), October (Lmp13), and November (Lmp15). The highest deposition values (>1.2 mmol C m⁻² d⁻¹) occurred between March and April (Lmp02), and in June (Lmp06), both periods were characterized by dry deposition (Fig.2 and Table 2). High DOC fluxes (>0.6 mmol C m⁻² d⁻¹) were, however, also observed in March (Lmp01), May (Lmp04) and at the end of July (Lmp10), in correspondence with periods dominated by wet deposition. In 2015, the annual rainfall was 360 mm, slightly higher than the average annual rainfall for the island of Lampedusa (325 mm with 42 days of rain), (data from: <http://www.arpa.sicilia.it/> and <http://www.eurometeo.com/italian/climate>).

177

178

179

180

181

In 2016, the DOC deposition rates were rather low and with less variability compared to the previous year. DOC fluxes ranged between 0.1 and 0.3 mmol C m⁻² d⁻¹ from January to May (Lmp18 to Lmp23), and from June to August (Lmp27 to Lmp30). The highest DOC fluxes (>0.8 mmol C m⁻² d⁻¹) were observed in May (Lmp25) and between October and November (Lmp33; Fig. 2 and Table 2). In 2016, the annual rainfall was 378 mm (data from the local meteorological station of the Lampedusa Atmospheric Observatory).

182

183

184

185

186

187

188

In 2017, DOC fluxes ranged between 0.14 and 0.92 mmol C m⁻² d⁻¹, from January to April (Lmp36 to Lmp41); these values are higher than those observed in the first three months of the previous year (Fig. 2 and Table 2).

Atmospheric fluxes of DOC in wet deposition were correlated with monthly precipitation rates ($r^2=0.47$, $p<0.05$, $n=12$). The precipitation rate ranged between 2.9 and 88.5 mm during the study period (2015-2017).

A mean daily deposition of 0.33 mmol C m⁻² d⁻¹ was calculated, taking into consideration the two years (from March 2015 to April 2017), corresponding to an annual DOC flux of 120.7 mmol C m⁻² year⁻¹.

189

3.2 DON and TDN, DOP and TDP atmospheric fluxes

190

191

192

193

Dissolved Nitrogen fluxes ranged between 1.5·10⁻³ and 0.25 mmol DON m⁻² d⁻¹ and between 1.6·10⁻³ and 0.47 mmol TDN m⁻² d⁻¹, respectively (Fig. 3 and Table 2). During most of the sampling period (93%), DON deposition was lower than 0.1 mmol m⁻² d⁻¹. The main peaks were observed in March 2015 (Lmp01), in May (Lmp24 and Lmp25) and October 2016 (Lmp33) coinciding with high DOC deposition (Fig. 3 and Table 2).

194

195

196

Dissolved phosphorous fluxes ranged between 0 and 2.7·10⁻³ mmol DOP m⁻² d⁻¹ and 1·10⁻⁴ and 5·10⁻³ mmol TDP m⁻² d⁻¹, respectively (Fig. 4 and Table 2). Between August 2015 and September 2016 (Lmp10-Lmp30) both DOP and TDP showed low fluxes. In 2015, atmospheric DOP and TDP showed the highest fluxes in May (Lmp04) and August

197 (Lmp10). In 2016, the main peaks in DOP and TDP deposition were observed in October (Lmp31) and November
198 (Lmp33). The 4 peaks in atmospheric DOP and TDP (Lmp04, Lmp10, Lmp31 and Lmp33) were responsible for 16% of
199 total depositions coinciding with high DOC fluxes (Fig. 2). It is noteworthy that in March 2015 (Lmp01) and May 2016
200 (Lmp25), DOP fluxes were very low (0 and $9 \cdot 10^{-5}$ mmol m⁻² d⁻¹, respectively) (Table 2), despite high fluxes of DOC,
201 DON and TDP.

202 The overall mean DON and DOP daily deposition rates were 0.032 mmol N m⁻² d⁻¹ and $3.8 \cdot 10^{-4}$ mmol P m⁻² d⁻¹,
203 corresponding to annual fluxes of 11.61 mmol DON m⁻² y⁻¹ and 0.14 mmol DOP m⁻² y⁻¹.

204 It should be noted that these fluxes could be underestimated due to the missing samples in 2015 and 2016.

205

206 3.3 Elemental ratios in atmospheric DOM

207 DOC:DON:DOP ratios showed a marked variability (Fig. 5 and Table 3). DOC:DON molar ratios ranged between 2.2
208 (Lmp24, May 2016) and 45.9 (Lmp04, May 2015) (Fig. 5a). DOC:DOP molar ratios ranged between 244 (Lmp10,
209 August 2015) and 11008 (Lmp25, May 2016) (Fig. 5b). DON:DOP ratio ranged between 9.2 (Lmp10, August 2015)
210 and 1377 (Lmp25, May 2016) (Fig. 5c). No clear seasonal cycle was observed, even if during autumn (November 2015
211 and October 2016) and late spring (May 2016) depositions were very low in P, compared to the other two elements.

212

213 3.4 The sources of atmospheric DOM

214 Previous works indicate that soluble fractions of V and Ni in aerosol samples are specific marker for anthropogenic
215 sources for the area of Lampedusa (Becagli et al, 2012 and 2017). During this study, samples did not show enrichment
216 beyond 10, indicating that their source is mainly from crustal origin.

217 The DOC deposition was classified on the basis of the corresponding nssCa concentration in PM₁₀, (Following Marconi
218 et al., 2014) (Fig. 6). Saharan dust events are identified as those with nssCa > 950 ng/m³. DOC deposition,
219 corresponding to average nssCa larger than the threshold (950 ng/mg³), is highlighted in red. DOC deposition,
220 corresponding to a Saharan dust event occurring in at least one day of the sampling period, is indicated in yellow (Fig.
221 6). A detailed description of the most interesting deposition events is given below.

222 The mean concentration of PM₁₀ for Lmp01 (March 2015) was 50.1 μg m⁻³, with an average dust value of 18.2 μg m⁻³
223 (Table 4). This sample is dominated by crustal input as revealed by the values of nssCa in the aerosol (1327.6 ng/m³)
224 and the Al concentration in the deposition (both soluble and particulate, Fig. 7). In this sample EF(Pb) indicates low
225 contribution of anthropogenic sources. Na concentration in the deposition was 304 mg m⁻² d⁻¹ (Fig. 7).

226 Lmp02 (March-April 2015) is characterized by the second highest DOC deposition, although no Saharan dust event
227 occurred during this period (Fig. 6 and 7). The PM₁₀ mean concentration was 29 μg m⁻³ and average sea-salt aerosol
228 value was 13.6 μg m⁻³ (Table 4) with a 47% contribution to PM₁₀. This sample was strongly affected by sea spray as
229 indicated by the Na/Al ratio 60-fold higher than in Lmp01.

230 Lmp04 (May 2015), sampled during a Saharan dust event, also showed high DOC input (Fig. 6), but the concentration
231 of Al in the deposition was quite low (Fig. 7). The PM₁₀ mean concentration was 26.4 μg m⁻³ and the average sea-salt in
232 the aerosol was 8.8 μg m⁻³, contributing by one third to the total particulate matter. As for Lmp03 the ratio Na/Al is
233 quite high suggesting that sea spray also dominated in this sample.

234 The mean PM₁₀ concentration of Lmp06 (June 2015), was 23.3 μg m⁻³, with an average sea-salt aerosol concentration of
235 13.6 μg m⁻³ (Table 4). The average contribution of sea salt aerosol to the particulate matter concentration was 27%. The

236 peculiar characteristic of this sample is the high concentration of soluble Al and low particulate Al in the deposition
237 (Fig. 7). This feature is also observed in samples Lmp10 and Lmp12, both presenting quite high concentration of DOC
238 in July and September 2015.

239 Lmp25 (May 2016) was characterized by a mean PM_{10} concentration of $133.7 \mu\text{g m}^{-3}$ and with an average dust value of
240 $42.5 \mu\text{g m}^{-3}$ (Table 4). This is the highest value of PM_{10} observed in the entire study and indicates the occurrence of a
241 Saharan dust event. The average value of nssCa was 4815.1 ng/m^3 , further supporting the occurrence of an intense
242 Saharan dust event. The Saharan dust contribution for this sample is also revealed by the Al concentration (both soluble
243 and particulate) (Fig. 7).

244 Lmp33 (October-November 2016) and Lmp34 (November 2016) are indicative of the two possible source of DOC,
245 crustal and sea spray. Lmp33 shows higher DOC concentration than Lmp34. The former is characterized by very high
246 Na concentration in the deposition, while Lmp34 is characterized by high crustal content (as revealed by the high
247 concentration of Al, Fig. 7).

248 The fourth highest DOC deposition of the entire study period (Lmp37) occurred in January 2017. Unfortunately no
249 ancillary data was collected during this event.

250

251 **4. Discussion**

252 **4.1 DOC input from the atmosphere**

253 The relationship between monthly precipitation rates and DOC fluxes confirmed the importance of rain events in the
254 Med Sea, (Djaoudi et al., 2018).

255 The total DOC annual input from the atmosphere ($120.7 \text{ mmol C m}^{-2} \text{ y}^{-1}$) found in this study, is very close to that
256 measured at Cap Ferrat peninsula (Southern France) in 2006 ($129 \text{ mmol C m}^{-2} \text{ y}^{-1}$; Pulido-Villena et al., 2008) and in
257 three lakes in the western Mediterranean basin (Southern Spain, $153.3 \text{ mmol C m}^{-2} \text{ y}^{-1}$ in 2005; De Vicente et al., 2012).

258 This value is higher than deposition in the north-western Med Sea ($59 \text{ mmol C m}^{-2} \text{ y}^{-1}$ at Frioul Island in the Bay of
259 Marseille; Djaoudi et al., 2018). If the same sampling period is taken into consideration for both studies (from March
260 2015, the beginning of sampling in Lampedusa, to July 2016, the end of sampling at Frioul island), DOC input is 2-
261 times higher at Lampedusa than at Frioul Island. This variability is probably due to the different temporal and seasonal
262 cycles of dry and wet deposition. In particular the marked differences between the two sites could be influenced by the
263 presence of a south-north decreasing gradient in the intensity of the mineral dust deposition as proposed by Vincent et
264 al. (2016). Our data also show high variability in DOC deposition rates without a clear seasonality. While in 2015 and
265 2016 the highest deposition rates were between spring and autumn, in 2017 the highest deposition rates were in winter.
266 In addition the two highest peaks observed in 2015 (Lmp02 and Lmp06, dry deposition) accounted together for 43% of
267 the annual DOC flux ($52 \text{ mmol C m}^{-2} \text{ y}^{-1}$). Depending on the origin and trajectories of the air masses, the atmosphere
268 can carry significant amounts of DOC.

269 Assuming that the annual DOC flux from this study ($120.7 \text{ mmol C m}^{-2} \text{ y}^{-1}$) is valid for the whole Med Sea
270 (area= $2.5 \cdot 10^{12} \text{ m}^2$), we can estimate a total input of $3.64 \text{ Tg DOC y}^{-1}$. The global estimation for wet atmospheric DOC
271 deposition is $306\text{-}580 \text{ Tg C y}^{-1}$ and the input to the global ocean ranges between 90 and 246 Tg C y^{-1} (Willey et al.,
272 2000; Kanakidou et al., 2012). The global dry deposition of organic carbon (OC) has been estimated to be 11 Tg C y^{-1} ,
273 (Jurado et al., 2008) leading to a total OC deposition to the oceans of $101\text{-}247 \text{ Tg C y}^{-1}$. The comparison of these

274 estimates indicates that the Med Sea, with an area equivalent to only 0.7% of the global oceans, receives from 1.5 to 4%
275 of the global atmospheric input of DOC.

276 It is noteworthy that, our values are up to 6 times larger than the estimate of the total river input to the Med Sea (0.6-0.7
277 Tg DOC y^{-1} ; Santinelli, 2015). These results confirm the leading role of atmosphere in the transport of allochthonous
278 DOC to the Med Sea, as suggested recently by Santinelli et al. (2015) and Galletti et al. (2019).

279 A few episodes of Saharan outbreaks can strongly affect the annual dust flux, whereby a single outbreak can account for
280 40-80% of the flux (Guerzoni et al., 1997). The most intense dust deposition events in Lampedusa generally display
281 higher values in spring (March-June) and in autumn (Vincent et al., 2016; Bergametti et al., 1989; Loye-Pilot and
282 Martin, 1996; Avila et al., 1997; Ternon et al., 2010). In this study, we show that, although dust events can significantly
283 contribute to the annual DOC fluxes, sea spray seems the dominant source of DOC in this area, in agreement with
284 Mallet et al., 2019. The role of secondary organic aerosols as a source of organic matter in the Mediterranean Sea is
285 well documented (Arndt et al., 2017; Michoud et al., 2017; Rinaldi et al., 2017) and could be relevant at Lampedusa.
286 Finally, the correlation between monthly precipitation rates and DOC fluxes shows the importance of rain events as a
287 source of DOC in the Med Sea, as proposed by Djaoudi et al. (2018).

288

289 **4.2 Atmospheric DON, DOP input and elemental ratios**

290 The annual DON flux (11.61 mmol N $m^{-2} y^{-1}$) observed at Lampedusa was lower than that measured at Frioul Island
291 (17.80 mmol N $m^{-2} y^{-1}$; Djaoudi et al., 2018). In the Eastern Med Sea, Markaki et al. (2010) reported a DON annual flux
292 of 18.49 mmol N $m^{-2} y^{-1}$, higher than that observed at Lampedusa. The comparison of our DOP deposition values (0.14
293 mmol P $m^{-2} y^{-1}$) with the few data reported in the literature shows that the fluxes at Lampedusa are markedly higher
294 than those reported for the Western Med Sea (0.07 mmol P $m^{-2} y^{-1}$, Djaoudi et al., 2018; 0.03 mmol P $m^{-2} y^{-1}$, Migon
295 and Sandroni, 1999), but lower than those obtained by Violaki et al. (2017) for both the West (1.16 mmol P $m^{-2} y^{-1}$) and
296 East (0.90 mmol P $m^{-2} y^{-1}$) Med Sea. Results from our study are very similar to those reported for the Eastern Med Sea
297 in 2001 and 2002 (0.15 mmol P $m^{-2} y^{-1}$) (Markaki et al., 2010). Further, it is interesting to note that our DOP data are
298 very similar to the TDP data reported for a coastal rural site in the NE Spain in 2002-2003 (0.10-0.14 mmol P $m^{-2} y^{-1}$, in
299 17 months of sampling; Izquierdo et al., 2012).

300 Over the entire time-series, the average DOP and DON contributions to TDP and TDN were 40% and 26%,
301 respectively. These data confirm that a significant fraction of the dissolved P and N in the atmospheric deposition was
302 in the organic form. These values are similar to those observed in previous studies at Frioul Island (DOP 40%, DON
303 25%; Djaoudi et al., 2018), and in both the western and eastern Med Sea (DOP 38%; DON 32%; Markaki et al., 2010).
304 The similarity among the depositions collected at the two sites (Lampedusa, Central Med Sea and Frioul, North-western
305 Med Sea) suggests that the remote site of Lampedusa may be representative of DON and DOP deposition in the Med
306 Sea, especially in the western basin.

307 The data on atmospheric elemental ratios show that each deposition event is characterized by a specific elemental ratio,
308 suggesting a high variability in DOM composition and the presence of multiple sources. Djaoudi et al (2018) observed
309 an average value of DOC:DON:DOP molar ratios of 1228:308:1 in atmospheric DOM, collected in the north-western
310 Med Sea. In the surface Med Sea, DOC:DON:DOP ratios ranges between 1050:84:1 in the western basin to 1560:120:1
311 in the eastern basin (Pujo-Pay et al., 2011). The average values observed in our atmospheric deposition time-series
312 (1909:292:1) indicate that atmospheric DOM is enriched in DOC and DON compared to marine DOM. This

313 observation is also valid comparing our values with those recently measured on marine samples collected at the
314 MOOSE ANTARES offshore station (north-western Med Sea) (1227:100:1, Djaoudi et al., 2018).

315 All the analyzed samples, except few cases in summer 2016, are relative to dry+wet deposition (Table 1). Although the
316 DON and DOP recorded during the dry period are generally on the low end side of the measured range (Table 2), no
317 information on the role played by wet or dry deposition on DON and DOP input to the Med Sea can be drawn at this
318 stage, due to the limited number of dry samples.

319

320 **4.3 The contribution of Saharan dust to atmospheric fluxes of dissolved organic carbon**

321 The input of Saharan dust can affect the chemistry of the Mediterranean aerosols and enrich the Med Sea with many
322 elements (such as Co, Ni, trace metals). Very few studies are available on the interactions between organic carbon and
323 Saharan dust, even though the organic material found in the troposphere is often associated with dust particles (Usher et
324 al., 2003; Aymoz et al., 2004).

325 Our results show that Saharan dust events can represent a relevant, albeit intermittent, source of DOC to the central Med
326 Sea. Focusing on the different peaks of DOC deposition, our results indicate that Lmp01, Lmp04 and Lmp25 are
327 associated to a Saharan dust event and that aerosols were probably enriched with organic substances. We hypothesize
328 that dust particles present in the aerosol adsorb organic molecules, facilitating their accumulation and transport (Usher
329 et al., 2003). The role of Saharan dust in the transport of DOC is evident in Lmp25 (May 2016).

330 In addition Lmp01 (end of March 2015), Lmp04 (May 2015) and Lmp25 (May 2016) show a seasonality that could be
331 linked to the transport of pollen attached to desert particles in the spring events, and this pollen would contribute to
332 atmospheric DOC input in spring (end of March- May). Pollen originating in Morocco was detected in South Spain
333 (Cabezudo et al., 1997) and various pollen types (Cannabis, Cupressus, Pinus, Platanus and Sambucus) were observed
334 in Cordoba (South Spain) exclusively during dust African events (Cariñanos et al., 2004). This process would not occur
335 in the other seasons (winter and autumn of no pollen production).

336 If all the Saharan dust deposition events (red and yellow in Fig. 6) are taken into account, an input of 49.58 mmol DOC
337 m⁻² to Lampedusa can be estimated, representing ~41% of the total DOC flux for the entire sampling period. The strong
338 dust events (red in Fig. 6) lead a flux of 15.26 mmol DOC m⁻², representing 13% of the total flux. Each deposition event
339 must be considered individually, as DOC content depends on the aerosol load (Formenti et al., 2003; Aymoz et al.,
340 2004).

341 Wet deposition is the main driver of Saharan dust deposition to the Med Sea. However, dry deposition can be also
342 important (Guerzoni et al., 1997) and its relative contribution strongly depends on meteorological conditions and local
343 emission (Inomata et al., 2009). Some models have estimated that wet deposition represents up to 75-95% of total
344 deposition (Iavorivska et al., 2016). While our results confirm the importance of wet deposition, it also stress the
345 relevance of dry deposition (32% of the total deposition during the entire sampling period) that appears to be the main
346 contributor of DOC and of other chemical species to the remote site of Lampedusa, as suggested by Morales-Baquero et
347 al. (2013).

348 It is also evident that Saharan dust input is not always associated with high DOC input as seen in Lmp34, with high
349 concentration of dust, but with low DOC concentration. Conversely, several samples (for example Lmp02, Lmp33 and
350 Lmp37) characterized by high concentrations of DOC, do not show high crustal content. Indeed high DOC deposition
351 events seems to be often associated to sea spray transport, (Lmp02, Lmp10, Lmp 12, Lmp 33 and Lmp 37; Fig. 6).

352 Similarly, samples Lmp01, Lmp04, Lmp10, Lmp12 and especially Lmp25, also show a large contribution of sea spray
353 aerosol indicating a marine source for the DOC in these samples. This is a surprising result, because other studies (e.g.,
354 Pace et al., 2006) have shown that clean marine aerosol conditions are rare at Lampedusa.
355 Lmp23, Lmp27, Lmp32, Lmp35 and Lmp36 were not characterized by high DOC fluxes (Fig. 6), even if these
356 sampling periods were characterized by at least one strong Saharan dust event (Fig. 6, in yellow). This observation
357 supports the hypothesis that Saharan dust is not typically enriched with DOC, but it adsorbs organic molecules in the
358 atmosphere, and depending on its route, can be enriched or not in DOC. The composition of sample Lmp34 further
359 supports this hypothesis, with the third highest average nss Ca value (1092.2 ng/m^3), but with a DOC concentration
360 ($0.20 \text{ mmol m}^{-2} \text{ d}^{-1}$) below the daily average flux of the entire sampling period ($0.33 \text{ mmol m}^{-2} \text{ d}^{-1}$) (Fig. 6, Tables 2 and
361 4).
362 Lastly, it is interesting to note that samples characterized by high values of DOC never present high EF(Pb). Samples
363 presenting $\text{EF(Pb)} > 10$ show very low DOC concentrations, indicating a small DOC contribution from anthropogenic
364 aerosols at Lampedusa.

365

366 **4.4 Implications for marine ecosystem**

367 The measurements carried out at the Island of Lampedusa clearly show that the atmosphere is an important source of
368 allocthonous DOC to the Central Med Sea. There is still little information on biological lability of atmospheric DOC; if
369 it is biologically available, it can be used very quickly by marine prokaryotic heterotrophs and it can be channeled into
370 the food web, whereas if it is mainly recalcitrant, it can accumulate and be transported by water masses circulation.

371 A conceptual exercise can be made in order to give an estimate of the implications of DOM deposition for marine
372 ecosystem. According to D'Ortenzio et al. (2005), mixed layer depth (MLD) ranges between 15 and 30 m, close to the
373 island of Lampedusa. Santinelli et al. (2012) observed an average mixed layer DOC concentration of $60 \mu\text{M}$ in the same
374 area in September 1999, and estimated a bacterial carbon demand (BCD) of $0.32 \mu\text{M C d}^{-1}$ (assuming a bacterial growth
375 efficiency of 15%), which represents the total amount of carbon needed to support the observed bacterial production. In
376 September, the atmospheric DOC flux was $0.24 \text{ mmol C m}^{-2} \text{ d}^{-1}$ in 2015 and $0.38 \text{ C m}^{-2} \text{ d}^{-1}$ in 2016. Dividing the
377 atmospheric deposition by the average MLD (22.5 m, D'Ortenzio et al. 2005), we estimate that the atmospheric input
378 contributes to $0.011\text{-}0.017 \mu\text{M DOC d}^{-1}$ increase in the mixed layer. Assuming that the values of BCD observed in
379 September 1999 ($0.32 \mu\text{M C d}^{-1}$) are valid also for September 2015 and 2016, and that all the DOC coming from the
380 atmosphere is labile, it could satisfy 3-5% of the daily BCD. During summer the MLD varies between 10 and 15 m
381 depth, with an average value of 12.5 m (D'Ortenzio et al. 2005). The DOC input from the atmosphere is expected to
382 increase the DOC concentration in the mixed layer by $0.008\text{-}0.079 \mu\text{M C d}^{-1}$ from June to August 2015, and by 0.013-
383 0.014 from June to August 2016, supplying 3-25% of the daily BCD, assuming similar DOC concentrations and
384 bacterial activity as during September. Even if we are aware that these assumptions are hardly meet, in particular the
385 estimate of DOC input to the whole Med Sea, based on the data collected in Lampedusa, we think that these
386 calculations can give an idea of the relevant role that atmospheric input of DOC can have in sustaining heterotrophic
387 prokaryotes productivity in the surface layer, particularly when the upper water column is strongly stratified.

388 The Mediterranean MLD seasonal variability is characterized by a basin scale deepening from November to February-
389 March and an abrupt stratification in April, which is maintained throughout the summer and early autumn. Even if these
390 estimates stress the potential role of atmospheric DOC in sustaining bacterial productivity in the surface ocean, a time

391 series of BCD, MLD and DOC concentrations in the surface layer, together with a network of stations for the
392 quantification of atmospheric input of DOC in the different areas of the Med Sea, are mandatory in order to have an
393 accurate estimate of the impact of DOC atmospheric on the functioning of marine ecosystem. It should be also noted
394 that a fraction of atmospheric DOC could be recalcitrant, and through transport to depth, it could play a key role in
395 carbon sequestration. The refractory nature of a part of atmospheric DOM has been proposed by Sánchez-Pérez et al.
396 (2016), based on a 2-year time series data on Fluorescent DOM (FDOM) deposition in the North-western Med Sea
397 (Barcelona coastal area, Spain). Their results show that atmospheric inputs induced changes in the quality of organic
398 matter, increasing the proportion of FDOM substances in the DOM pool. Incubation experiments to investigate the
399 biological lability of atmospheric DOC are also crucial to better understand the impact of atmospheric deposition on
400 marine ecosystems.

401 Finally, the occurrence of Saharan dust events opens interesting considerations on their impact on the marine
402 environment. Previous studies suggested that dust inputs can promote autotrophic production (Ridame and Guieu, 2002;
403 Markaki et al., 2003). Instead Pulido-Villena et al. (2008) experimentally found that heterotrophic bacteria can reduce
404 the amount of C exported to deeper waters, because a Saharan dust event would have induced the mineralization of 22-
405 70% of bioavailable DOC, changing carbon sequestration.

406

407 **4. Conclusions**

408 Our data show that atmospheric input has a larger impact to the Med Sea than to the global ocean and DOC fluxes from
409 the atmosphere to the Med Sea can be up to 6-fold larger than riverine input.

410 Organic substances transported by Saharan dust at Lampedusa are primarily of natural origin, in particular from sea
411 spray. Saharan dust can be an important carrier of organic substances. However, the load of DOC associated with dust
412 is highly variable and high DOC fluxes were observed also in absence of dust deposition events.

413 Atmospheric C:N:P molar ratios indicate that DOM is enriched in DOC and DON with respect to marine DOM and the
414 contribution of atmospheric deposition to the marine DOM stoichiometry in the Med Sea could be relevant, in particular
415 during stratified periods.

416 Further studies are needed to understand the link between atmospheric inputs and marine biogeochemistry. Data on
417 stable carbon ($\delta^{13}\text{C}$) on atmospheric DOC would be crucial in order to gain information about its main sources.
418 Incubation experiments should be carried out, both with aerosol rich or poor in DOC, in order to better understand how
419 the microbial community can respond to dust input. Further studies are also needed to understand the link between
420 aerosol origin and DOM concentration and quality, and to comprehend the potential link between DOC and the pollen
421 during the spring. Lastly, longer time series combined with a modelling effort, would provide a solid base to assess the
422 response of DOM dynamics in the Med Sea to changes in aerosol deposition pattern due to the effect of climate change.

423

424 **Author contribution**

425 YG and CS conceived of the study and the sampling design. YG, SB, DMS collected the samples. YG, MG, SB, RT,
426 SV analyzed the samples. YG, CS, EPV, AdS analyzed the data and all authors assisted with data discussion and
427 contributed to the revision and editing of the final manuscript. All authors are aware of and accept responsibility for this
428 manuscript and have approved the final submitted manuscript.

429

430 **Acknowledgements**

431 Part of this research was supported by “Professionalità” project, funded by the *Fondazione Banca del Monte di*
432 *Lombardia*. The authors thank the analytical platform PACEM (Mediterranean Institute of Oceanography) for the
433 analysis of organic and inorganic forms of nitrogen. Contributions from Lorenzo De Silvestri and Francesco
434 Monteleone are gratefully acknowledged.

435

436 *The authors declare that they have no conflict of interest.*

437

438 *The dataset generated for this study are available on request to the corresponding author.*

439

440 **References**

- 441 Armstrong, F. A. J., Williams, P. M., and Strickland, J. H.: Photo-oxidation of organic matter in sea water by ultra-
442 violet radiation, analytical and other applications, *Nature*, 211(5048), 481, <https://doi.org/10.1038/211481a0>,
443 1966.
- 444 Aminot, A., and K erouel, R.: Dosage automatique des nutriments dans les eaux marines: m ethodes en flux continu,
445 Editions Quae, 2007.
- 446 Arndt, J., Sciare, J., Mallet, M., Roberts, G. C., Marchand, N., Sartelet, K., Sellegri, K., Dulac, F., Healy, R. M., and
447 Wenger, J. C.: Sources and mixing state of summertime background aerosol in the north-western Mediterranean
448 basin, *Atmos. Chem. Phys.*, 17, 6975–7001, <https://doi.org/10.5194/acp-17-6975-2017>, 2017.
- 449 Aymoz, G., Jaffrezo, J. L., Jacob, V., Colomb, A., and George, C.: Evolution of organic and inorganic components of
450 aerosol during a Saharan dust episode observed in the French Alps, *Atmospheric Chemistry and Physics*,
451 4(11/12), 2499-2512, <https://doi.org/10.5194/acp-4-2499-2004>, 2004.
- 452 Avila, A., Queralt-Mitjans, I., and Alarc on, M.: Mineralogical composition of African dust delivered by red rains over
453 northeastern Spain. *Journal of Geophysical Research: Atmospheres*, 102(D18), 21977-21996,
454 <https://doi.org/10.1029/97JD00485>, 1997.
- 455 Becagli, S., Ghedini, C., Peeters, S., Rottiers, A., Traversi, R., Udisti, R., Chiari, M., Jalba, A., Despi au, S., Dayan, U.,
456 and Temara, A.: MBAS (Methylene Blue Active Substances) and LAS (Linear Alkylbenzene Sulphonates) in
457 Mediterranean coastal aerosols: sources and transport processes, *Atmospheric environment*, 45(37), 6788-6801,
458 <https://doi.org/10.1016/j.atmosenv.2011.04.041>, 2011.
- 459 Becagli, S., Sferlazzo, D. M., Pace, G., di Sarra, A., Bommarito, C., Calzolari, G., Ghedini, C., Lucarelli, F., Meloni, D.,
460 Monteleone, F., Severi, M., Trasversi, R., and Udisti, R.: Evidence for heavy fuel oil combustion aerosols from
461 chemical analyses at the island of Lampedusa: a possible large role of ships emissions in the Mediterranean,
462 *Atmospheric Chemistry and Physics*, 12(7), 3479-3492, <https://doi.org/10.5194/acp-12-3479-2012>, 2012.
- 463 Becagli, S., Lazzara, L., Fani, F., Marchese, C., Traversi, R., Severi, M., di Sarra, A., Sferlazzo, D. M., Piacentino, S.,
464 Bommarito, C., Dayan, U., and Udisti, R.: Relationship between methanesulfonate (MS⁻) in atmospheric
465 particulate and remotely sensed phytoplankton activity in oligo-mesotrophic central Mediterranean Sea,
466 *Atmospheric Environment*, 79, 681-688, <https://doi.org/10.1016/j.atmosenv.2013.07.032>, 2013.
- 467 Becagli, S., Anello, F., Bommarito, C., Cassola, F., Calzolari, G., Iorio, T. D., di Sarra, A., G omez-Amo, J. -L.,
468 Lucarelli, F., Marconi, M., Meloni, D., Monteleone, F., Nava, S., Pace, G., Severi, M., Sferlazzo, D. M.,
469 Traversi, R., and Udisti, R.: Constraining the ship contribution to the aerosol of the central Mediterranean,
470 *Atmospheric Chemistry and Physics*, 17(3), 2067-2084, <https://doi.org/10.5194/acp-17-2067-2017>, 2017.
- 471 Bergametti, G., Dutot, A. L., Buat-Menard, P., Losno, R., and Remoudaki, E.: Seasonal variability of the elemental
472 composition of atmospheric aerosol particles over the northwestern Mediterranean, *Tellus B*, 41(3), 353-361,
473 <https://doi.org/10.1111/j.1600-0889.1989.tb00314.x>, 1989.

- 474 Cabezudo, B., Recio, M., Sánchez-Laulhé, J., Trigo, M. D. M., Toro, F. J., and Polvorinos, F.: Atmospheric
475 transportation of marihuana pollen from North Africa to the southwest of Europe. *Atmospheric Environment*,
476 31(20), 3323-3328, [https://doi.org/10.1016/S1352-2310\(97\)00161-1](https://doi.org/10.1016/S1352-2310(97)00161-1), 1997.
- 477 Calzolari, G., Nava, S., Lucarelli, F., Chiari, M., Giannoni, M., Becagli, S., Trasversi, R., Marconi, M., Frosini, D.,
478 Severi, M., Udisti, R., di Sarra, A., Pace, G., Meloni, D., Bommarito, C., Monteleone, F., Anello, F., and
479 Sferlazzo, D. M.: Characterization of PM 10 sources in the central Mediterranean, *Atmospheric Chemistry and
480 Physics*, 15(24), 13939-13955, <https://doi.org/10.5194/acp-15-13939-2015>, 2015.
- 481 Cariñanos, P., Galan, C., Alcázar, P., and Dominguez, E.: Airborne pollen records response to climatic conditions in
482 arid areas of the Iberian Peninsula, *Environmental and Experimental Botany*, 52(1), 11-22,
483 <https://doi.org/10.1016/j.envexpbot.2003.11.008>, 2004.
- 484 D'Ortenzio, F., Iudicone, D., de Boyer Montegut, C., Testor, P., Antoine, D., Marullo, S., Santoleri, R., and Madec, G.:
485 Seasonal variability of the mixed layer depth in the Mediterranean Sea as derived from in situ profiles,
486 *Geophysical Research Letters*, 32(12), <https://doi.org/10.1029/2005GL022463>, 2005.
- 487 De Vicente, I., Ortega-Retuerta, E., Morales-Baquero, R., and Reche, I.: Contribution of dust inputs to dissolved
488 organic carbon and water transparency in Mediterranean reservoirs, *Biogeosciences* 9, 5049-5060,
489 <https://doi.org/10.5194/bg-9-5049-2012>, 2012.
- 490 Djaoudi, K., Van Wambeke, F., Barani, A., Hélias-Nunige, S., Sempéré, R., and Pulido-Villena, E.: Atmospheric fluxes
491 of soluble organic C, N, and P to the Mediterranean Sea: Potential biogeochemical implications in the surface
492 layer, *Progress in Oceanography*, 163, 59-69, <https://doi.org/10.1016/j.pocean.2017.07.008>, 2018.
- 493 Economou, C., and Mihalopoulos, N.: Formaldehyde in the rainwater in the eastern Mediterranean: occurrence,
494 deposition and contribution to organic carbon budget, *Atmospheric Environment* 36(8), 1337-1347,
495 [https://doi.org/10.1016/S1352-2310\(01\)00555-6](https://doi.org/10.1016/S1352-2310(01)00555-6), 2002.
- 496 Formenti, P., Elbert, W., Maenhaut, W., Haywood, J., Osborne, S., and Andreae, M. O.: Inorganic and carbonaceous
497 aerosols during the Southern African Regional Science Initiative (SAFARI 2000) experiment: Chemical
498 characteristics, physical properties, and emission data for smoke from African biomass burning, *Journal of
499 Geophysical Research: Atmospheres*, 108(D13), <https://doi.org/10.1029/2002JD002408>, 2003.
- 500 Galletti, Y., Gonnelli, M., Retelletti Brogi, S., Vestri, S., and Santinelli, C.: DOM dynamics in open waters of the
501 Mediterranean Sea: New insights from optical properties, *Deep Sea Research Part I: Oceanographic Research
502 Papers*, 144, 95-114, <https://doi.org/10.1016/j.dsr.2019.01.007>, 2019.
- 503 Goudie, A. S., and Middleton, N. J.: Saharan dust storms: nature and consequences, *Earth-science reviews*, 56(1-4),
504 179-204, [https://doi.org/10.1016/S0012-8252\(01\)00067-8](https://doi.org/10.1016/S0012-8252(01)00067-8), 2001.
- 505 Guerzoni, S., and Chester, R. (Eds.): *The impact of desert dust across the Mediterranean (Vol. 11)*, Springer Science &
506 Business Media, Netherlands, 1996.
- 507 Guerzoni, S., Molinaroli, E., and Chester, R.: Saharan dust inputs to the western Mediterranean Sea: depositional
508 patterns, geochemistry and sedimentological implications, *Deep Sea Research Part II: Topical Studies in
509 Oceanography*, 44(3), 631-654, [https://doi.org/10.1016/S0967-0645\(96\)00096-3](https://doi.org/10.1016/S0967-0645(96)00096-3), 1997.
- 510 Henderson, P., and Henderson, G.M. (Eds.): *The Cambridge Handbook of Earth Science Data*. University Press,
511 Cambridge, 2009.
- 512 Hansell, D.A.: Dissolved organic carbon reference material program. *Eos, Transactions American Geophysical Union*
513 86(35), 318-318, <https://doi.org/10.1029/2005EO350003>, 2005.
- 514 Herut B., Collier R., and Krom M.D.: The role of dust in supplying nitrogen and phosphorus to the South East
515 Mediterranean, *Limnology and Oceanography*, 47:870-878, <https://doi.org/10.4319/lo.2002.47.3.0870>, 2002.
- 516 Iavorivska, L., Boyer, E. W., and DeWalle, D. R.: Atmospheric deposition of organic carbon via precipitation,
517 *Atmospheric Environment*, 146, 153-163, <https://doi.org/10.1016/j.atmosenv.2016.06.006>, 2016.
- 518 Inomata, Y., Igarashi, Y., Chiba, M., Shinoda, Y., and Takahashi, H.: Dry and wet deposition of water-insoluble dust
519 and water-soluble chemical species during spring 2007 in Tsukuba, Japan, *Atmospheric Environment*, 43(29),
520 4503-4512, <https://doi.org/10.1016/j.atmosenv.2009.06.048>, 2009.
- 521 IPCC (Eds.): *Climate change: mitigation of climate change*, In: Edenhofer, O., Pichs-Madruga, R., Sokona, Y.,
522 Farahani, E., Kadner, S., Seyboth, K., Adler, A., Baum, I., Brunner, S., Eickemeier, P., Kriemann, B.,
523 Savolainen, J., Schlömer, S., von Stechow, C., Zwickel, T., and Minx, J. C., *Contribution of working group III to
524 the fifth assessment report of the intergovernmental panel on climate change*, Cambridge University Press,
525 Cambridge, 2014.
- 526 Izquierdo, R., Benítez-Nelson, C. R., Masqué, P., Castillo, S., Alastuey, A., and Àvila, A.: Atmospheric phosphorus
527 deposition in a near-coastal rural site in the NE Iberian Peninsula and its role in marine productivity,
528 *Atmospheric environment*, 49, 361-370, <https://doi.org/10.1016/j.atmosenv.2011.11.007>, 2012.
- 529 Jurado, E., Dachs, J., Duarte, C. M., and Simo, R.: Atmospheric deposition of organic and black carbon to the global
530 oceans, *Atmospheric Environment*, 42(34), 7931-7939, <https://doi.org/10.1016/j.atmosenv.2008.07.029>, 2008.
- 531 Kanakidou, M., Duce, R. A., Prospero, J. M., Baker, A. R., Benitez-Nelson, C., Dentener, F. J., Hunter, K. A., Liss, P.
532 S., Mahowald, N., Okin, G. S., Sarin, M., Tsigaridis, K., Uematsu, M., Zamora, L. M., and Zhu, T.: Atmospheric

533 fluxes of organic N and P to the global ocean, *Global Biogeochemical Cycles* 26(3),
534 <https://doi.org/10.1029/2011GB004277>, 2012.

535 Lai, A. M., Shafer, M. M., Dibb, J. E., Polashenski, C. M., and Schauer, J. J.: Elements and inorganic ions as source
536 tracers in recent Greenland snow, *Atmospheric Environment*, 164, 205–215, 2017.

537 Loÿe-Pilot, M. D., and Martin, J. M. (Eds.): Saharan dust input to the western Mediterranean: an eleven years record in
538 Corsica, In *The impact of desert dust across the Mediterranean* (pp. 191-199), Springer, Dordrecht, 1996.

539 Marconi, M., Sferlazzo, D. M., Becagli, S., Bommarito, C., Calzolari, G., Chiari, M., di Sarra, A., Ghedini, C.,
540 Gómez-Amo, J. L., Lucarelli, F., Meloni, D., Monteleone, F., Nava, S., Pace, G., Piacentino, S., Rugi, F.,
541 Severi, M., Traversi, R., and Udisti, R.: Saharan dust aerosol over the central Mediterranean Sea: PM10
542 chemical composition and concentration versus optical columnar measurements, *Atmos. Chem. Phys.*, 14,
543 2039–2054, <https://doi.org/10.5194/acp-14-2039-2014>, 2014.

544 Mallet, M. D., D'Anna, B., Mème, A., Bove, M. C., Cassola, F., Pace, G., Desboeufs, K., Di Biagio, C., Doussin, J.-F.,
545 Maille, M., Massabò, D., Sciare, J., Zapf, P., di Sarra, A. G., and Formenti, P.: Summertime surface PM1 aerosol
546 composition and size by source region at the Lampedusa island in the central Mediterranean Sea, *Atmos. Chem.*
547 *Phys.*, 19, 11123–11142, <https://doi.org/10.5194/acp-19-11123-2019>, 2019.

548 Markaki, Z., Oikonomou, K., Kocak, M., Kouvarakis, G., Chaniotaki, A., Kubilay, N., and Mihalopoulos, N.:
549 Atmospheric deposition of inorganic phosphorus in the Levantine Basin, eastern Mediterranean: Spatial and
550 temporal variability and its role in seawater productivity, *Limnology and Oceanography*, 48(4), 1557-1568,
551 <https://doi.org/10.4319/lo.2003.48.4.1557>, 2003.

552 Markaki, Z., Loÿe-Pilot, M. D., Violaki, K., Benyahya, L., and Mihalopoulos, N.: Variability of atmospheric deposition
553 of dissolved nitrogen and phosphorus in the Mediterranean and possible link to the anomalous seawater N/P
554 ratio, *Marine Chemistry*, 120(1-4), 187-194, <https://doi.org/10.1016/j.marchem.2008.10.005>, 2010.

555 Mermex group (Eds.): White book of Mermex program, *Progress in Oceanography*, 91, 97-166,
556 <https://doi.org/10.1016/j.pcean.2011.02.003>, 2011.

557 Michoud, V., Sciare, J., Sauvage, S., Dusanter, S., Léonardis, T., Gros, V., Kalogridis, C., Zannoni, N., Féron, A., Petit,
558 J.-E., Crenn, V., Baisnée, D., Sarda-Estève, R., Bonnaire, N., Marchand, N., DeWitt, H. L., Pey, J., Colomb, A.,
559 Gheusi, F., Szidat, S., Stavroulas, I., Borbon, A., and Locoge, N.: Organic carbon at a remote site of the western
560 Mediterranean Basin: sources and chemistry during the ChArMEx SOP2 field experiment, *Atmos. Chem. Phys.*,
561 17, 8837–8865, <https://doi.org/10.5194/acp-17-8837-2017>, 2017.

562 Migon, C., Copin-Montegut, G., Elegant, L., and Morelli, J.: Atmospheric input of nutrients to the coastal
563 Mediterranean area, *Biogeochemical implications*, *Oceanologica acta*. Paris, 12(2), 187-191, 1989.

564 Migon, C., and Sandroni, V.: Phosphorus in rainwater: Partitioning inputs and impact on the surface coastal ocean,
565 *Limnology and Oceanography*, 44(4), 1160-1165, <https://doi.org/10.4319/lo.1999.44.4.1160>, 1999.

566 Morales-Baquero, R., Pulido-Villena, E., and Reche, I.: Chemical signature of Saharan dust on dry and wet atmospheric
567 deposition in the south-western Mediterranean region, *Tellus B: Chemical and Physical Meteorology*, 65(1),
568 18720, <https://doi.org/10.3402/tellusb.v65i0.18720>, 2013.

569 Murphy, J., and Riley, J. P.: A modified single solution method for the determination of phosphate in natural water,
570 *Analytica chimica acta*, 27, 31-36, [https://doi.org/10.1016/S0003-2670\(00\)88444-5](https://doi.org/10.1016/S0003-2670(00)88444-5), 1962.

571 Pace, G., Meloni, D., and di Sarra, A.: Forest fire aerosol over the Mediterranean basin during summer 2003, *Journal*
572 *Geophys. Res.*, 110, D21202, <https://doi.org/doi:10.1029/2005JD005986>, 2005.

573 Pace, G., di Sarra, A., Meloni, D., Piacentino, S., and Chamard, P.: Optical properties of aerosols over the central
574 Mediterranean, 1. Influence of transport and identification of different aerosol types, *Atmos. Chem. Phys.*, 6,
575 697–713, 2006.

576 Prospero, J. M., Blades, E., Mathison, G., and Naidu, R.: Interhemispheric transport of viable fungi and bacteria from
577 Africa to the Caribbean with soil dust, *Aerobiologia*, 21(1), 1-19, <https://doi.org/10.1007/s10453-004-5872-7>,
578 2005.

579 Pulido-Villena, E., Wagener, T., and Guieu, C.: Bacterial response to dust pulses in the western Mediterranean:
580 Implications for carbon cycling in the oligotrophic ocean, *Global Biogeochemical Cycles*, 22(1),
581 <https://doi.org/10.1029/2007GB003091>, 2008.

582 Pujo-Pay, M., Conan, P., and Raimbault, P.: Excretion of dissolved organic nitrogen by phytoplankton assessed by wet
583 oxidation and 15N tracer procedures, *Marine Ecology Progress Series*, 153, 99-111,
584 <https://doi.org/10.3354/meps153099>, 1997.

585 Pujo-Pay, M., Conan, P., Oriol, L., Cornet-Barthaux, V., Falco, C., Ghiglione, J. F., Goyet, C., Moutin T., and Prieur,
586 L.: Integrated survey of elemental stoichiometry (C, N, P) from the western to eastern Mediterranean Sea, 2011.

587 Ridame, C., and Guieu, C.: Saharan input of phosphate to the oligotrophic water of the open western Mediterranean
588 Sea, *Limnology and Oceanography*, 47(3), 856-869, <https://doi.org/10.4319/lo.2002.47.3.0856>, 2002.

589 Rinaldi, M., Gilardoni, S., Paglione, M., Sandrini, S., Decesari, S., Zanca, N., Marinoni, A., Cristofanelli, P., Bonasoni,
590 P., and Ielpo, P.: Physico-chemical characterization of Mediterranean background aerosol at the Capogranitola

591 observatory (Sicily), EGU General Assembly Conference Abstracts, 23–28 April 2017, Vienna, Austria, 3161,
592 2017.

593 Rodríguez, S., Alastuey, A., Alonso-Pérez, S., Querol, X., Cuevas, E., Abreu-Afonso, J., Viana, M., Pérez, N., Pandolfi,
594 M., De la Rosa, J.: Transport of desert dust mixed with North African industrial pollutants in the subtropical
595 Saharan Air Layer, *Atmospheric Chemistry & Physics*, 11(13), <http://dx.doi.org/10.5194/acp-11-6663-2011>,
596 2011.

597 Sánchez-Pérez, E. D., Marín, I., Nunes, S., Fernández-González, L., Peters, F., Pujo-Pay, M., Conan, P., Marrasé, C.:
598 Aerosol inputs affect the optical signatures of dissolved organic matter in NW Mediterranean coastal waters,
599 *Scientia Marina* 80(4), 437-446, <https://doi.org/10.3989/scimar.04318.20B>, 2016.

600 Santinelli, C., Sempéré, R., Van Wambeke, F., Charriere, B., and Seritti, A.: Organic carbon dynamics in the
601 Mediterranean Sea: An integrated study, *Global Biogeochemical Cycles*, 26(4), 2012.

602 Santinelli, C.: DOC in the Mediterranean Sea. In: Hansell D.A, Carlson C.A. (Eds.), *Biogeochemistry of Marine*
603 *Dissolved Organic Matter* (Second edition), Academic Press, San Diego, pp. 579-608,
604 <https://doi.org/10.1016/B978-0-12-405940-5.00013-3>, 2015.

605 Santinelli, C., Follett, C., Brogi, S. R., Xu, L., and Repeta, D.: Carbon isotope measurements reveal unexpected cycling
606 of dissolved organic matter in the deep Mediterranean Sea, *Marine Chemistry*, 177, 267-277,
607 <https://doi.org/10.1016/j.marchem.2015.06.018>, 2015.

608 Sellitto, P., Zanetel, C., di Sarra, A., Salerno, G., Tapparo, A., Meloni, D., Pace, G., Caltabiano, T., Briole, P., and
609 Legras, B.: The impact of Mount Etna sulfur emissions on the atmospheric composition and aerosol properties in
610 the central Mediterranean: a statistical analysis over the period 2000-2013 based on observations and Lagrangian
611 modelling, *Atmos. Environ.*, 148, 77-88, 2017.

612 Ternon, E., Guieu, C., Loÿe-Pilot, M. D., Leblond, N., Bosc, E., Gasser, B., Miquel, J. -C., and Martín, J.: The impact
613 of Saharan dust on the particulate export in the water column of the North Western Mediterranean Sea,
614 *Biogeosciences*, 7(3), 809-826, <https://doi.org/10.5194/bg-7-809-2010>, 2010.

615 Usher, C. R., Michel, A. E., and Grassian, V. H.: Reactions on mineral dust, *Chemical Reviews*, 103(12), 4883-4940,
616 2003.

617 Vincent, J., Laurent, B., Losno, R., Bon Nguyen, E., Rouillet, P., Sauvage, S., Chevaillier, S., Coddeville, P.,
618 Ouboulmane, N., di Sarra, A. G., Tovar-Sánchez, A., Sferlazzo, D. M., Massanet, A., Triquet, S., Morales
619 Baquero, R., Fornier, M., Coursier, C., Desboeufs, K., Dulac, F., and Bergametti, G.: Variability of mineral dust
620 deposition in the western Mediterranean basin and south-east of France, *Atmospheric Chemistry and Physics*,
621 16(14), 8749-8766, <https://doi.org/10.5194/acp-16-8749-2016>, 2016.

622 Willey, J. D., Kieber, R. J., Eyman, M. S., and Avery, G. B.: Rainwater dissolved organic carbon: concentrations and
623 global flux, *Global Biogeochemical Cycles* 14(1), 139-148, <https://doi.org/10.1029/1999GB900036>, 2000.

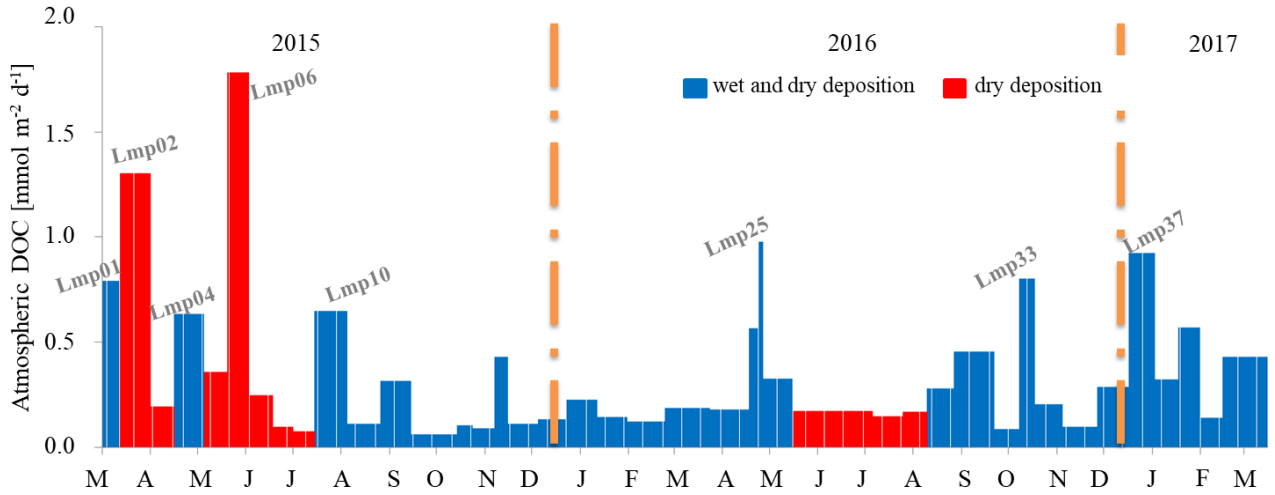
624



625
626

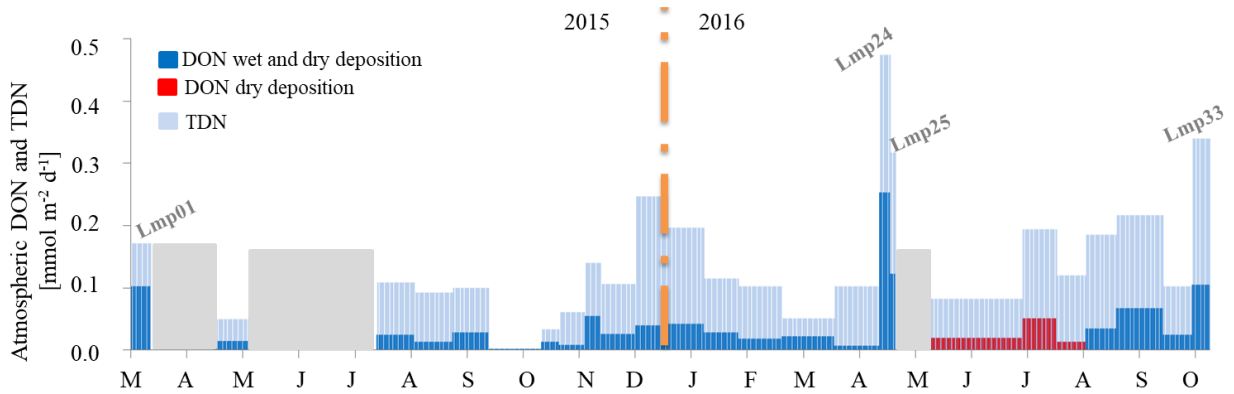
Figure 1: Sampling location (Lampedusa island 35.5° N, 12.6° E) and the total atmospheric deposition collector.

627



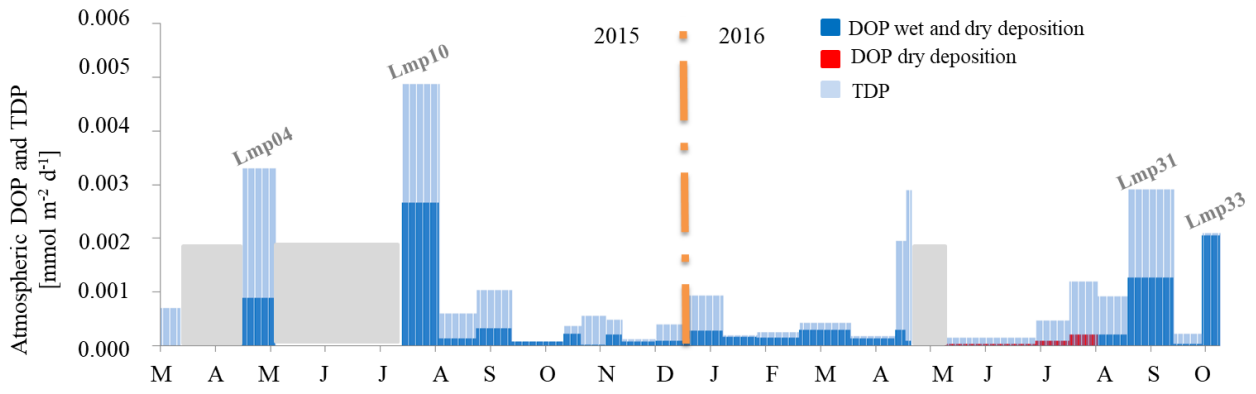
628
629
630
631
632

Figure 2: Atmospheric DOC fluxes during the study period. The month abbreviation and tick marks correspond to the end of the corresponding month. The width of the bar refer to the length of the sampling period. Wet and dry deposition is indicated in blue, dry deposition in red.

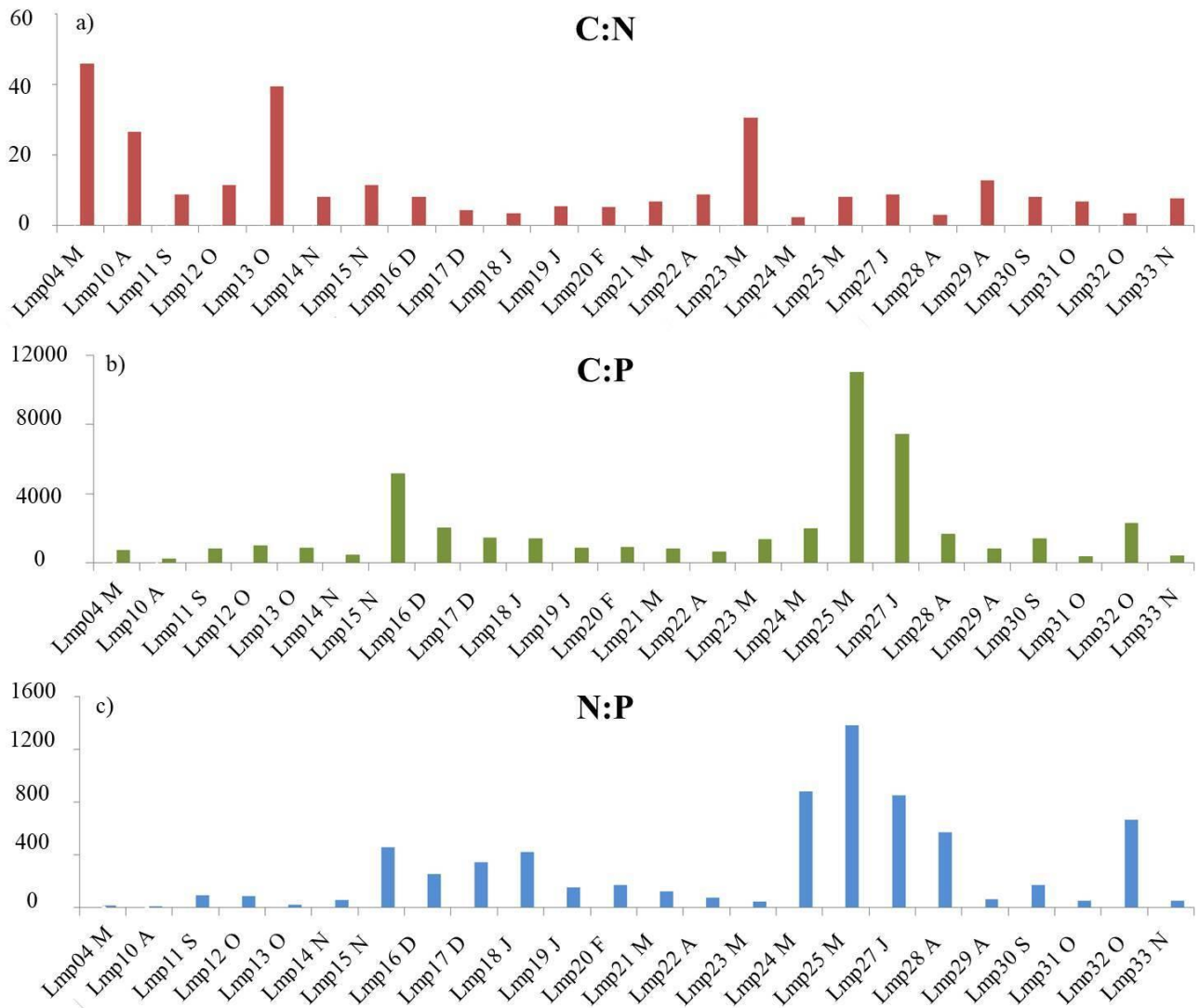


633
634
635
636

Figure 3. Atmospheric DON and TDN deposition. Grey areas correspond to the periods with no data. The month abbreviation and tick marks correspond to the end of the corresponding month. The width of the bar refer to the length of the sampling period.

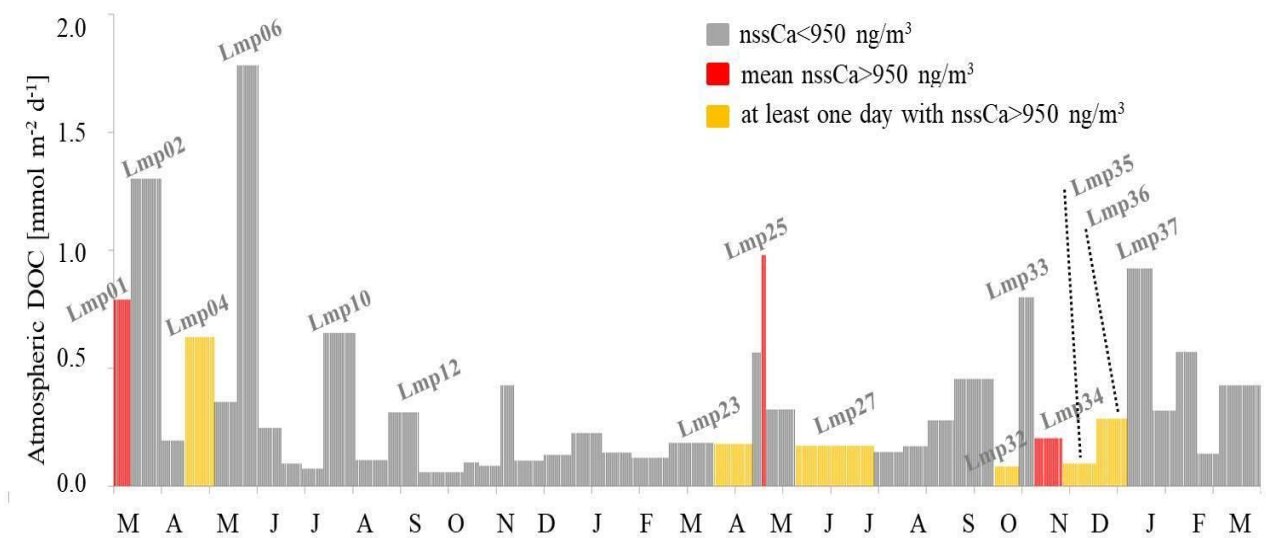


637
 638 **Figure 4. Atmospheric DOP and TDP deposition** Grey areas correspond to the periods with no data. The month
 639 **abbreviation and tick marks correspond to the end of the corresponding month. The width of the bar**
 640 **refer to the length of the sampling period.**
 641



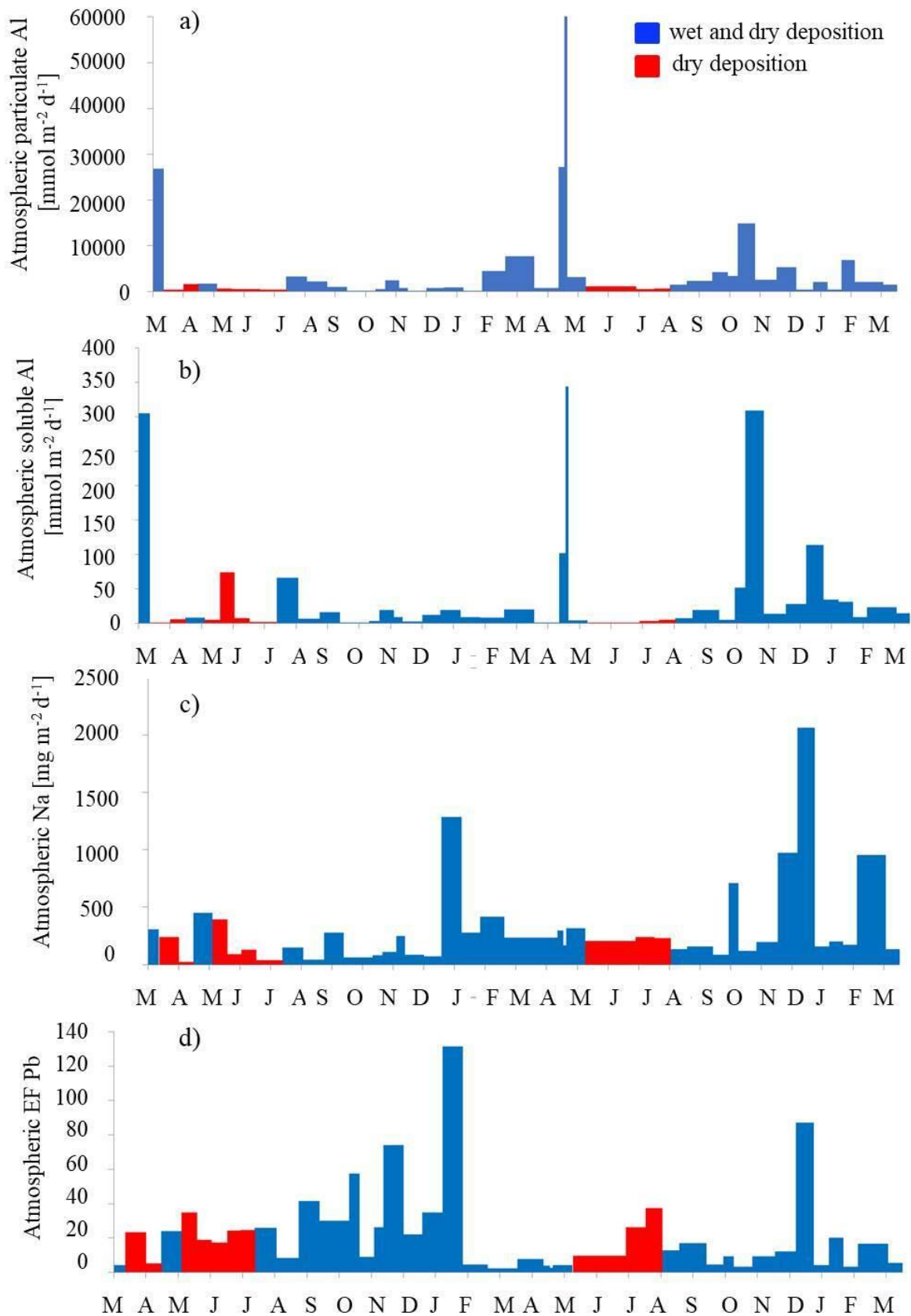
642
643
644
645

Figure 5. Temporal evolution of C:N (a), C:P (b) and N:P (c) ratios in atmospheric deposition samples. Sample name and the initials of each month (from March, Lmp04, to November, Lmp33) are reported in the X-axis.



646
647
648
649
650

Figure 6. Temporal dynamics in the dust deposition events during the sampling period color coded based on the contribution of non-sea salt Ca (nssCa). The month abbreviation and tick marks correspond to the end of the corresponding month. The width of the bar refer to the length of the sampling period.



651
 652 **Figure 7. Temporal dynamics of atmospheric particulate Aluminium (a), soluble Aluminium (b), soluble Sodium**
 653 **(c) and enrichment factor for Lead (d). The month abbreviation and tick marks correspond to the end of**
 654 **the corresponding month. The width of the bar refer to the length of the sampling period.**

Sample name	Sampling period			Deposition type	Volume collected [L]
	Start date	End date	Total days		
Lmp01	18/03/2015	28/03/2015	10	wet and dry	6
Lmp02	28/03/2015	17/04/2015	20	dry	0.26
Lmp03	17/04/2015	02/05/2015	16	dry	0.27
Lmp04	02/05/2015	21/05/2015	19	wet and dry	1.8
Lmp05	21/05/2015	05/06/2015	15	dry	0.28
Lmp06	05/06/2015	19/06/2015	15	dry	0.29
Lmp07	19/06/2015	04/07/2015	16	dry	0.26
Lmp08	04/07/2015	17/07/2015	14	dry	0.26
Lmp09	17/07/2015	31/07/2015	14	dry	0.27
Lmp10	31/07/2015	21/08/2015	20	wet and dry	9
Lmp11	21/08/2015	11/09/2015	22	wet and dry	2
Lmp12	11/09/2015	01/10/2015	20	wet and dry	5
Lmp13	01/10/2015	30/10/2015	29	wet and dry	0.5
Lmp14	30/10/2015	09/11/2015	11	wet and dry	2
Lmp15	09/11/2015	23/11/2015	14	wet and dry	0.6
Lmp16	23/11/2015	02/12/2015	9	wet and dry	1.2
Lmp17	02/12/2015	21/12/2015	19	wet and dry	1.9
Lmp18	21/12/2015	08/01/2016	18	wet and dry	1.8
Lmp19	08/01/2016	28/01/2016	20	wet and dry	6.1
Lmp20	28/01/2016	16/02/2016	19	wet and dry	2.7
Lmp21	16/02/2016	11/03/2016	26	wet and dry	2.1
Lmp22	11/03/2016	09/04/2016	28	wet and dry	7.1
Lmp23	09/04/2016	04/05/2016	26	wet and dry	0.3
Lmp24	04/05/2016	10/05/2016	6	wet and dry	2.3
Lmp25	10/05/2016	13/05/2016	3	wet and dry	1.9
Lmp26	13/05/2016	01/06/2016	19	wet and dry	0.7
Lmp27	01/06/2016	22/07/2016	50	dry	0.26
Lmp28	22/07/2016	10/08/2016	19	dry	0.24
Lmp29	10/08/2016	26/08/2016	16	dry	0.24
Lmp30	26/08/2016	12/09/2016	17	wet and dry	0.8
Lmp31	12/09/2016	08/10/2016	26	wet and dry	12
Lmp32	08/10/2016	24/10/2016	16	wet and dry	0.5
Lmp33	24/10/2016	03/11/2016	10	wet and dry	11
Lmp34	03/11/2016	21/11/2016	18	wet and dry	12
Lmp35	21/11/2016	13/12/2016	22	wet and dry	1.7
Lmp36	13/12/2016	02/01/2017	20	wet and dry	9.5
Lmp37	02/01/2017	19/01/2017	17	wet and dry	6.5
Lmp38	19/01/2017	03/02/2017	15	wet and dry	1.5
Lmp39	03/02/2017	17/02/2017	14	wet and dry	5
Lmp40	17/02/2017	03/03/2017	14	wet and dry	0.75

Lmp41	03/03/2017	01/04/2017	29	wet and dry	5.5
-------	------------	------------	----	-------------	-----

656 **Table 1. Sampling period, type of deposition and volume for the 41 samples collected at the Island of**
657 **Lampedusa.**

658

Sample name	DOC fluxes [mmol m ⁻² d ⁻¹]	DON fluxes [mmol m ⁻² d ⁻¹]	TDN fluxes [mmol m ⁻² d ⁻¹]	DOP fluxes [mmol m ⁻² d ⁻¹]	TDP fluxes [mmol m ⁻² d ⁻¹]
Lmp01	0.80	0.10	0.17	0	7·10 ⁻⁴
Lmp02	1.30	n.a.	n.a.	n.a.	n.a.
Lmp03	0.19	n.a.	n.a.	n.a.	n.a.
Lmp04	0.63	0.01	0.05	9·10 ⁻⁴	3·10 ⁻³
Lmp05	0.36	n.a.	n.a.	n.a.	n.a.
Lmp06	1.78	n.a.	n.a.	n.a.	n.a.
Lmp07	0.25	n.a.	n.a.	n.a.	n.a.
Lmp08	0.10	n.a.	n.a.	n.a.	n.a.
Lmp09	0.07	n.a.	n.a.	n.a.	n.a.
Lmp10	0.65	0.02	0.11	3·10 ⁻³	5·10 ⁻³
Lmp11	0.11	0.01	0.09	1·10 ⁻⁴	6·10 ⁻⁴
Lmp12	0.31	0.03	0.10	3·10 ⁻⁴	1·10 ⁻³
Lmp13	0.06	1.5·10 ⁻³	1.6·10 ⁻³	7·10 ⁻⁵	8·10 ⁻⁵
Lmp14	0.10	0.01	0.03	2·10 ⁻⁴	4·10 ⁻⁴
Lmp15	0.09	8·10 ⁻³	0.06	2·10 ⁻⁵	6·10 ⁻⁴
Lmp16	0.43	0.05	0.14	2·10 ⁻⁴	5·10 ⁻⁴
Lmp17	0.11	0.03	0.11	7·10 ⁻⁵	1·10 ⁻⁴
Lmp18	0.13	0.04	0.25	9·10 ⁻⁵	4·10 ⁻⁴
Lmp19	0.23	0.04	0.20	3·10 ⁻⁴	9·10 ⁻⁴
Lmp20	0.14	0.03	0.12	2·10 ⁻⁴	2·10 ⁻⁴
Lmp21	0.12	0.02	0.10	2·10 ⁻⁴	3·10 ⁻⁴
Lmp22	0.18	0.02	0.05	3·10 ⁻⁴	4·10 ⁻⁴
Lmp23	0.18	6·10 ⁻³	0.10	1·10 ⁻⁴	2·10 ⁻⁴
Lmp24	0.57	0.25	0.47	3·10 ⁻⁴	2·10 ⁻³
Lmp25	0.98	0.12	0.32	9·10 ⁻⁵	3·10 ⁻³
Lmp26	0.33	n.a.	n.a.	n.a.	n.a.
Lmp27	0.17	0.02	0.08	2·10 ⁻⁵	1·10 ⁻⁴
Lmp28	0.14	0.05	0.19	9·10 ⁻⁵	5·10 ⁻⁴
Lmp29	0.17	0.01	0.12	2·10 ⁻⁴	1·10 ⁻³
Lmp30	0.28	0.04	0.18	2·10 ⁻⁴	9·10 ⁻⁴
Lmp31	0.45	0.07	0.22	1·10 ⁻³	3·10 ⁻³
Lmp32	0.08	0.02	0.10	4·10 ⁻⁵	2·10 ⁻⁴
Lmp33	0.80	0.10	0.34	2·10 ⁻³	2·10 ⁻³
Lmp34	0.20	n.a.	n.a.	n.a.	n.a.
Lmp35	0.10	n.a.	n.a.	n.a.	n.a.
Lmp36	0.29	n.a.	n.a.	n.a.	n.a.
Lmp37	0.92	n.a.	n.a.	n.a.	n.a.
Lmp38	0.32	n.a.	n.a.	n.a.	n.a.
Lmp39	0.57	n.a.	n.a.	n.a.	n.a.
Lmp40	0.14	n.a.	n.a.	n.a.	n.a.
Lmp41	0.43	n.a.	n.a.	n.a.	n.a.

659 **Table 2. Atmospheric fluxes of DOC, DON, TDN, DOP and TDP at the Island of Lampedusa.**

660

Sample	Sampling date	C:N	C:P	N:P
Lmp01	28/03/2015	7.78	n.a.	n.a.
Lmp04	21/05/2015	45.87	715.08	15.59
Lmp10	21/08/2015	26.57	244.38	9.20
Lmp11	11/09/2015	8.67	807.94	93.15
Lmp12	01/10/2015	11.37	977.79	85.98
Lmp13	30/10/2015	39.44	864.07	21.91
Lmp14	09/11/2015	8.02	449.04	56.00
Lmp15	23/11/2015	11.26	5131.65	455.83
Lmp16	02/12/2015	7.97	2036.66	255.42
Lmp17	21/12/2015	4.24	1448.37	341.90
Lmp18	08/01/2016	3.34	1406.60	420.55
Lmp19	28/01/2016	5.38	832.69	154.79
Lmp20	16/02/2016	5.09	882.80	173.40
Lmp21	11/03/2016	6.63	812.40	122.55
Lmp22	09/04/2016	8.78	645.65	73.53
Lmp23	04/05/2016	30.48	1353.57	44.41
Lmp24	10/05/2016	2.24	1976.03	882.33
Lmp25	13/05/2016	7.99	11008.94	1377.41
Lmp27	22/07/2016	8.73	7405.29	848.62
Lmp28	10/08/2016	2.89	1641.49	568.76
Lmp29	26/08/2016	12.66	796.68	62.95
Lmp30	12/09/2016	8.06	1376.27	170.77
Lmp31	08/10/2016	6.74	356.03	52.84
Lmp32	24/10/2016	3.41	2275.72	666.53
Lmp33	03/11/2016	7.68	389.57	50.73

661 **Table 3. C:N:P molar ratios in atmospheric DOM.**

662

Sample name	Mean PM₁₀ [µg/m³]	Mean sea salt aerosol [µg/m³]	Mean dust [µg/m³]	Mean nssCa [ng/m³]
Lmp01	50.1	13.0	18.2	1327.6
Lmp02	29.0	13.6	n.a.	62.2
Lmp03	28.1	9.8	n.a.	371.6
Lmp04	26.4	8.8	4	351.7
Lmp05	16.7	4.6	n.a.	87.3
Lmp06	23.1	6.1	n.a.	166.1
Lmp07	22.2	7.1	n.a.	139.3
Lmp08	26.5	5.4	n.a.	311.6
Lmp09	28.3	8.0	n.a.	188.2
Lmp10	29.1	5.2	3.4	492.7
Lmp11	n.a.	n.a.	n.a.	n.a.
Lmp12	n.a.	n.a.	n.a.	n.a.
Lmp13	n.a.	n.a.	n.a.	n.a.
Lmp14	n.a.	n.a.	n.a.	n.a.
Lmp15	n.a.	n.a.	n.a.	n.a.
Lmp16	n.a.	n.a.	n.a.	n.a.
Lmp17	n.a.	n.a.	n.a.	n.a.
Lmp18	n.a.	n.a.	n.a.	n.a.
Lmp19	n.a.	n.a.	n.a.	n.a.
Lmp20	n.a.	n.a.	n.a.	n.a.
Lmp21	n.a.	n.a.	n.a.	n.a.
Lmp22	n.a.	n.a.	n.a.	n.a.
Lmp23	39.5	18.3	3.8	488.1
Lmp24	30.7	18.7	1.2	154
Lmp25	133.7	15.5	42.5	4815.1
Lmp26	25.9	13.1	1.5	168.8
Lmp27	26.2	9.3	2.3	319.5
Lmp28	24.7	8.8	1.8	161.5
Lmp29	25	9.6	1.0	235.9
Lmp30	22.4	5.1	n.a.	330.8
Lmp31	24.5	5.6	n.a.	286.2
Lmp32	32.9	8.7	n.a.	772.5
Lmp33	31.8	11.8	n.a.	344.2
Lmp34	35.3	7.8	n.a.	1092.2
Lmp35	22.3	7.5	0.4	394
Lmp36	35.8	12.3	4.6	661.5
Lmp37	n.a.	n.a.	n.a.	n.a.
Lmp38	n.a.	n.a.	n.a.	n.a.
Lmp39	n.a.	n.a.	n.a.	n.a.
Lmp40	n.a.	n.a.	n.a.	n.a.

Lmp41	n.a.	n.a.	n.a.	n.a.
-------	------	------	------	------

663 **Table 4. The PM₁₀, sea salt aerosol, dust and nssCa mean values of the atmospheric total deposition.**